Investigation of the Structure of γ-Al_2O_3-Supported MgO by Surface Extended Energy Loss Fine Structure

Xiaohua Huang, Huizhong Huang,* Deen Jiang, and Biying Zhao

Institute of Physical Chemistry, Peking University, Beijing, 100871, P. R. China

Received: February 22, 2001; In Final Form: October 30, 2001

This study for the first time investigated the structure of a supported oxide system by SEELFS, the research of which had significance not only in the preparation of advanced solid base catalyst but also in the application of SEELFS technique onto a supported system. We present here the experimental results of a supported oxide system by SEELFS through the structural analysis of magnesia on a γ-alumina carrier. Using a fitting procedure based on an EXAFS-like formula and the phase shifts of a model compound of MgO, the coordination distances for Mg−O and Mg−Mg shells were obtained semiquantitatively and the coordination numbers obtained qualitatively. In addition, the contribution terms in the SEELFS oscillation of Mg K-edge of magnesia were also analyzed by the back Fourier transform of a corresponding Fourier function.

Introduction

A solid base is a widely considered catalyst for base-catalyzed homogeneous and heterogeneous catalysis reactions such as anionic polymerization,[1] aldol condensation,[2−4] alkylation,[5−7] Knoevenagel reaction,[8,9] and many other reactions.[10−12] Especially in the field of petroleum industry, a solid base was used in the process of mercaptan oxidation as a cocatalyst to convert RSH to innocuous disulfide.[13] The use of a solid base can avoid a lot of caustic aqueous bases. So, there has been increasing interest in the investigation of a solid base as a good environmental catalyst.[14] One kind of solid base considered is single-component metal oxides such as MgO and La_2O_3, which can provide enough basicity, but it is usually difficult to obtain large specific surface area and to adjust their pore structure. Another alternative kind is a mixed oxide like calcined hydrotalcite—Mg(Al)O, which has high surface area, moderate basicity, and structure stability. But in water the catalyst will be converted to pseudoboehmite, so the surface area and basicity decreased and activity decreased. In contrast, a supported oxide has many advantages. The catalyst has high surface area and pore structure through spontaneous dispersion of oxide on the carrier. In addition, the strength and the amount of basic sites can be adjusted by changing the type of the basic oxide and its loading amount. Another advantage is that the stability of a carrier like alumina is conducive to resist water and therefore may be helpful to increase the durability of the catalyst. Therefore, it is important to investigate a supported oxide catalyst. We consider alumina-supported magnesia because MgO is the most widely studied single-metal-oxide solid base[14] while alumina is the most commonly used carrier.

It is well know that many salt and oxides can disperse spontaneously onto the surfaces of a carrier to form a monolayer, and such a monolayer dispersion principle has been proved by XRD, XPS, Raman, EXAFS, TPD, TPR, etc.[15,16] The XRD result[17] showed that the dispersion of MgO on γ-Al_2O_3 is also a common monolayer dispersion phenomenon. Although there are some investigations on the basicity selection as well as activity of the MgO/γ−Al_2O_3 catalyst,[17−19] all these research studies did not refer to the basic structural aspect, which is more important to the design of an advanced catalyst.

The determination of surface atomic structural information is still one of the difficult problems in surface science. Methods of electron and X-ray diffraction have had a dominant role in these investigations over a long period. However, most of these structural techniques are not capable of providing direct information on the atomic geometry of the surface unit cell.[20] In recent years there have been interesting developments in spectroscopic methods for studying the local atomic structures that are based on analysis of extended oscillating structures of spectra. Among these, Extended X-ray Absorption Fine Structure (EXAFS)[21] is the best developed. It is currently used as a standard method for the analysis of local atomic structure. In the past few years it was shown that Surface Extended Energy Loss Fine Structures above ionization edges (SEELFS)[22−25] could be used for determining many structural parameters associated with the local surface environment. The SEELFS mechanism is similar to that of EXAFS and was systematically explained by Crescenzi.[25] Comparing to EXAFS and other EXAFS-like methods, we adopted the SEELFS technique on account of the main peculiarities of SEELFS including the fact that the experimental accessibility lies in low primary electron beam current (E_p = 10−3000 eV) to avoid surface sample heating and desorption, short time of surface structural acquisition data on surfaces, and materials without long-range order and simple data manipulation.

There has been no report on the investigation of SEELFS technique onto supported oxide because of the weaker SEELFS signal due to the low loading amount of supported materials. In this paper, we demonstrate the tenability on the lattice site of the SEELFS technique in the case of monolayer dispersion systems of γ-Al_2O_3−supported MgO by improving the signal-detecting mode and data-collecting mode. Through a fitting procedure using the EXAFS-like formula and the phase shifts of a model compound of MgO, we are able to investigate the structural information of MgO dispersed onto γ-Al_2O_3 carrier in semi-quantitative and qualitative ways. The accessibility of the SEELFS technique and the reasonability of the experimental

* Corresponding author. Fax: +86-10-62753937. E-mail: huanghz@csb0.ipc.pku.edu.cn.

10.1021/jp010712r CCC: $22.00
Published on Web 02/26/2002

results added a new proof for the well-known monolayer dispersion phenomenon.

Experimental Section

A. Preparation of MgO/γ-Al_2O_3. The preparation of MgO/γ-Al_2O_3 is similar to that described in another report.[17] The γ-Al_2O_3 carrier was obtained by calcining pseudoboehmite at 823 K for 5 h. MgO/γ-Al_2O_3 was prepared by impregnating the γ-Al_2O_3 with the solution of magnesium nitrate, followed by drying at 383 K overnight and calcining at 773 K for 4 h. Pure MgO indicated in this paper was obtained by calcining $Mg(NO_3)_2 \cdot 6H_2O$ at 773 K for 4 h.

For the SEELFS measurements, the powder MgO/γ-Al_2O_3 was pressed to thin slices with a thickness of 1 mm and diameter of 10 mm by a 769YP-24Z powder presser. The pressure was 15 MPa and the time of pressing was 5 min. Due to the insulation of the powder samples, there existed a shift of charge in the position of peaks. So, we used pure Cu foil to surround a MgO/γ-Al_2O_3 slice with a hole 2 mm in diameter to expose the samples for collection of data.

Because of the adsorption of water and carbon dioxide the MgO/γ-Al_2O_3 sample must be dried at 573 K for 3 h to get rid of adsorbed water, carbon dioxide, as well as any other impurity. After drying, the sample was immediately transferred to the Fast Entry Chamber of the Auger Electron Spectrometer at 373 K in order to keep the clean surface.

B. SEELFS Measurements. The experiments were performed with a PHI 3017 Auger Electron Spectrometer. The base pressure of the UHV Chamber was 10^{-10} Torr. The electron gun was coaxial to a single pass CMA (Cylindrical Mirror Analyzer), which was driven in the auger mode for detecting the SEELFS oscillations above the K edge of magnesium. The primary energy of incidence electrons was 1600 eV, with a beam current of 9.2 μA and a modulation of 10 V. On account of the weak SEELFS signal, the experimental data were collected as the electron yield of the first derivative electron yield using a lock-in amplifier to obtain the extended feature as far as possible from the core edge onset. The signal was cumulated through multi-time collection mode. The signal of the first derivative electron was converted to the numeric signal by a self-made V/F board and then collected by computer.

C. Analysis of Experimental Data. The original SEELFS signal in the form of electronic kinetic energy was first converted to the form of binding energy with self-compiled SEELFS PROCESSING procedure. We restricted our data range to eliminate features which were not directly associated with the SEELFS, mainly the core loss feature and the near-edge structure and extended the data range of 250 eV above the Mg K-edge energy so as to include all the available data. Because the theoretical SEELFS oscillation was composed of sine wave function, the SEELFS data was then converted from energy to wavenumber according to the following relation:

$$K(\text{Å}^{-1}) = \frac{\sqrt{2mE}}{\hbar} E = E_{\text{Loss}} - E_{\text{bind}} \qquad (1)$$

where E is the excited electron energy above the edge, E_{Loss} is the measured energy loss of the scattered electron, and E_{bind} is the binding energy of the core electron. To remove the background superimposed onto the SEELFS signal, the extended fine structure was isolated from the atomic structure μ_0 contribution with a spine function through the EXAFS-like procedure by the Chinese Academy of Physics.

To learn about the coordination distance, the SEELFS signal was transformed into a Fourier function according to the following equation:[25]

$$|F(R)| = \frac{1}{\sqrt{2\pi}} \int_{K_{\min}}^{K_{\max}} \chi(K)\omega(K)Ke^{-2iKR}\,\mathrm{d}K \qquad (2)$$

where $F(R)$ is the radial distribution function, $K_{\min}$ and $K_{\max}$ are the lower and upper limits of the data range, $\chi(K)$ is the experimental SEELFS signal in the wavenumber subtracted of background, R is the nearest-neighbor crystallographic distance, $\omega(K)$ is the window function multiplied to avoid truncation effects and spurious ripples in the FT analysis, and K is the weight function multiplied to correct the oscillatory term of the SEELFS so that all the K regions contribute with the same weight to the Fourier transform. As in EXAFS spectroscopy, the peaks in the SEELFS $F(R)$ do not correspond immediately to the crystallographic values. It should be corrected for a proper phase shift. We deduced the phase shift directly from the experiment using a model compound of MgO. The experimental phase shift could be used in all compounds of MgO/γ-Al_2O_3 because the same absorber and backscatter pair of atoms were involved.

We inversed the Fourier function to give a contribution to the original SEELFS spectrum of only the nearest Mg−O and Mg−Mg shell. The relation of the inversion is shown in eq (3):[25]

$$\chi_i(K) = \frac{1}{\sqrt{2\pi}} \int_{R_{\min}}^{R_{\max}} F_i(R)e^{2iKR}\,\mathrm{d}R \qquad (3)$$

We also deduced the experimental line of total phase shift versus wavenumber of the Mg−O and Mg−Mg shell, respectively, according to the following equation:[25]

$$\phi_1(K) = arctg\left(\frac{R_e[\chi_1(K)]}{I_m[\chi_1(K)]}\right) - 2KR_1 \qquad (4)$$

where R_1 is the nearest-neighbor crystallographic distance.

Results and Discussions

The XRD results in other report[17] showed that the dispersion of MgO on γ-Al_2O_3 was a monolayer dispersion phenomenon, with the threshold of 0.17 g MgO/g γ-Al_2O_3. To learn about the structural information of MgO on γ-Al_2O_3, the samples at 0.025, 0.08, and 0.23 g MgO/g γ-Al_2O_3 were selected for the SEELFS measurement. Due to the superimposing of the L edges of Mg and Al, which were both at approximately 74 eV while there had been no methods to separate them, so the Mg K edge selected was suitable for the SEELFS measurement with respect to MgO/γ-Al_2O_3 system.

The original SEELFS spectra above the Mg K edge for the MgO/γ-Al_2O_3 system are shown in Figure 1. The top curve is the pure MgO spectrum used as a model compound for correcting the phase shift of the coordination distance. The SEELFS data have been collected as a derivative of the electron yield using a modified lock-in amplifier to obtain the extended feature as for as possible from the core edge onset. The corresponding Fourier transforms are shown in Figure 2.

In the $F(R)$ function of MgO two prominent peaks are observed in the nearest neighbor at about 1.71 and 2.68 Å with errors of ±0.05 Å, which are assigned to the Mg−O and Mg−Mg peaks, respectively. The high errors are mainly due to the reduced $\Delta k = k_{\max} - k_{\min}$ range (typically 6−8 Å) in the

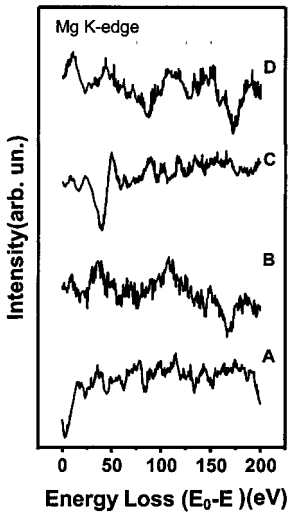

Figure 1. SEELFS spectra of (A) 0.025, (B) 0.08, (C) 0.23 g MgO/g γ-Al_2O_3, and (D) pure MgO. $E_p = 1600$ eV.

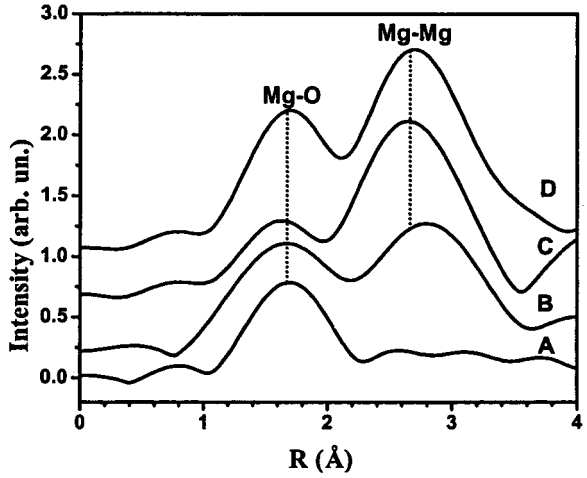

Figure 2. Fourier transforms of Mg K-edge SEELFS of γ-Al_2O_3-supported MgO with (A) 0.025, (B) 0.08, (C) 0.23 g MgO/g γ-Al_2O_3, and (D) pure MgO.

SEELFS data analysis and the noise in the original signals. The significant differences of these values with respect to the nearest-neighbor coordination distances of MgO, with the value of 2.10 and 2.97 Å, are mainly attributed to phase shifts of the electron waves from the central Mg atoms and the backscattering O and Mg atoms, respectively. As the same absorber atoms and backscatter atoms were involved in the MgO/γ-Al_2O_3 system, the experimental phase shift of pure crystalline MgO could be used for the correction of the Mg−O and Mg−Mg in alumina-supported MgO. The peak positions for the first two Mg−O and Mg−Mg shells of MgO/γ-Al_2O_3 after phase correction were obtained, shown in Table 1.

It can be seen from Table 1 and Figure 2 that with the increase of the MgO loading the positions of Mg−O peaks do not differ significantly, whereas there are significant differences in the positions of Mg−Mg peaks. Compared to crystalline MgO, the position of the Mg−Mg peak at 0.08 g MgO/g γ-Al_2O_3 increases by 0.13 Å which is beyond the experimental error. It can also be observed that there are no Mg−Mg peaks at 0.025 g MgO/g γ-Al_2O_3. In addition, the difference in the position of the Mg−Mg peaks between 0.23 g MgO/g γ-Al_2O_3 and crystalline MgO are within the range of errors. These results in the peak positions in the Fourier functions may indicate that the structures of Mg−O shells are not changed while those of Mg−Mg shells

TABLE 1: Interatomic Distances Measured by SEELFS with Crystallographic Data

no.	MgO loading amount	distance measured	length (Å)
A	0.025 g MgO/g γ-Al_2O_3	Mg−O	2.07 ± 0.05
		Mg−Mg	
B	0.08 g MgO/g γ-Al_2O_3	Mg−O	2.07 ± 0.05
		Mg−Mg	3.10 ± 0.05
C	0.23 g MgO/g γ-Al_2O_3	Mg−O	2.05 ± 0.05
		Mg−Mg	2.95 ± 0.05
D	MgO	Mg−O	2.10 ± 0.05
		Mg−Mg	2.97 ± 0.05

are changed by the dispersion of MgO onto γ-Al_2O_3. The disappearance in the second neighbor Mg peak at 0.025 g MgO/g γ-Al_2O_3 is because at a low loading amount of MgO, the MgO sites are more disordered or separated from one another and therefore the Mg−Mg peak cannot be observed. It should be noted that the data in Table 1 are not equal to the exact coordination distances due to the high errors so the results are just semiquantitative.

In addition, there are some qualitative results in coordination number. As the case in the EXAFS data analysis, peak height in $F(R)$ depends not only on the number of atoms coordinating the Mg atoms but also the disorder, which includes thermal disorder and structural disorder. In Figure 2, it can be seen that there were no significant differences in the peak heights for the Mg−O shells. The curve C has clearly a smaller Mg−O peak because of the noise. This is because as the nearest neighbor coordination relative to Mg atoms, the Mg−O bonding is strong and therefore is less susceptible to disordering, so, there is no variation in coordination number. For the Mg−Mg coordination, the disorder, especially the structural disorder, plays an important role in the peak heights. So, the variation in the peak height did not represent exactly the variation in the coordination number. But for sample C, whose loading amount of MgO on γ-Al_2O_3 is much higher than the threshold value, the SEELFS signal was just from surface crystalline MgO. As the crystalline MgO on γ-Al_2O_3 and the pure MgO powder are both long-range order, it can be assumed that the disorders are similar to each other. Therefore we expect that the same peak heights in samples C and D indicate the same coordination numbers. For sample B whose MgO loading is lower than the threshold of monolayer dispersion, the Mg−Mg peak height is much lower than that of pure MgO. One can estimate that the significant decrease in the peak height for Mg−Mg shell is due to the decrease in its coordination number.

The SEELFS signals before fourier transform and after back Fourier transform of the $F(R)$ between 0.8 and 3.8 Å are shown as solid and dotted line, respectively, in Figure 3.

From this graph, we can observe that the SEELFS signals after back Fourier transform of the $F(R)$ of pure crystalline MgO for Mg−O and Mg−Mg shell are in good agreement with those before fourier transform. This indicates that the SEELFS oscillations just come from the contribution of Mg−O and Mg−Mg shell. But for the alumina-supported MgO, there are some slight differences between them. One reason may be the effect of the alumina carrier. Another reason is the interference of the noise from locking amplifier. From the original SEELFS oscillation (in Figure 1), we can see that the noise is high. Although it can be separated from signals in the fitting process of the experimental data, it could not be completely eliminated.

Figures 4 and 5 are the relationship between phase shifts and the wave vectors for Mg−O and Mg−Mg shells in different samples. The great agreement between experimental results and fitting result indicates the reasonability of data analysis.

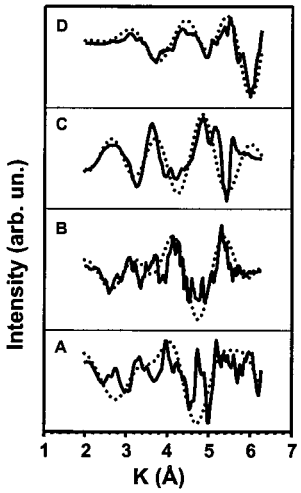

Figure 3. Solid line: SEELFS spectra after background subtraction of the original signals shown in Figure 1. Dotted line: SEELFS signal obtained after back Fourier inversion of the $F(R)$ shown in Figure 2.

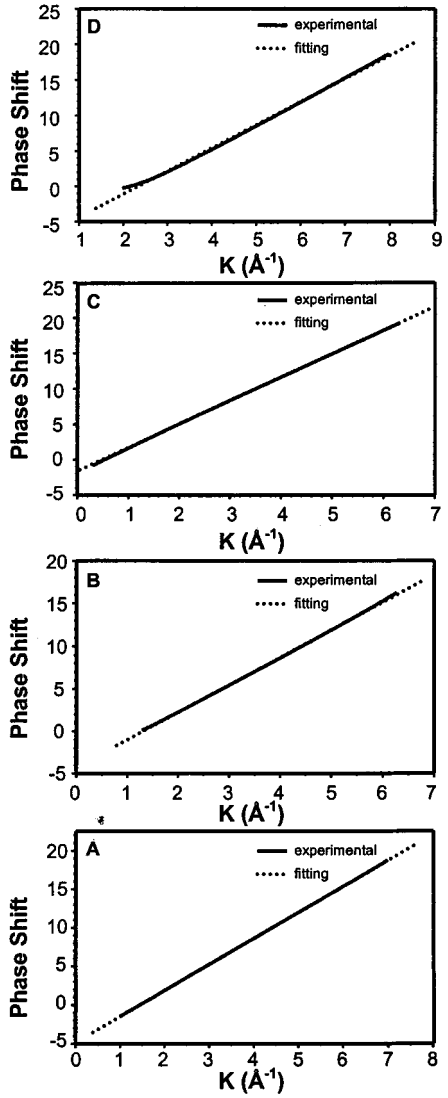

Figure 4. Relationship between the phase shifts and the wave-vectors of Mg−O in (A) 0.025, (B) 0.08, (C) 0.23 g/g γ-Al_2O_3, and (D) pure MgO.

Furthermore, the slope for the same shell in different samples in Table 2 is quite agreeable to each other.

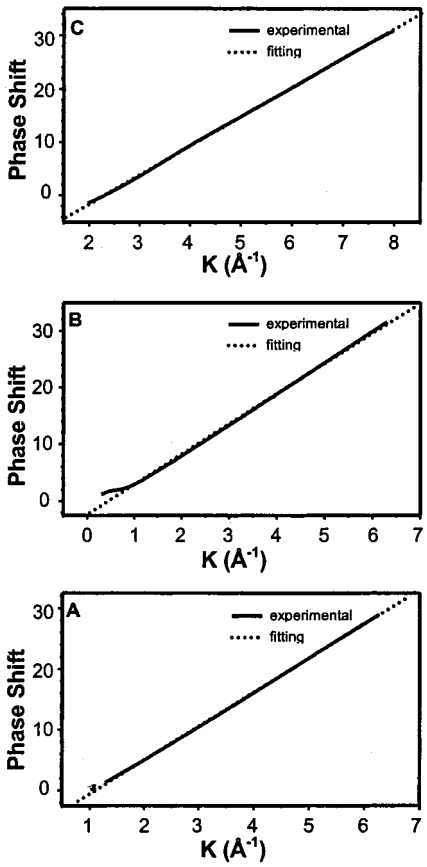

Figure 5. Relationship between the phase shifts and the vectors of wavenumber of Mg−Mg in (A) 0.08, (B) 0.23 g/g γ-Al_2O_3, and (C) pure MgO.

TABLE 2: The Slopes and Intercepts of Lines in Figure 4 and Figure 5

	MgO	Mg−O		Mg−Mg	
no.	loading amount	slope	intercept	slope	intercept
A	0.025 g MgO/g γ-Al_2O_3	3.372	−4.907		−6.2196
B	0.08 g MgO/g γ-Al_2O_3	3.232	−4.242	5.597	−2.254
C	0.23 g MgO/g γ-Al_2O_3	3.326	−1.7320	5.301	−12.681
D	MgO	3.257	−7.644	5.484	−6.2196

Conclusions

The Surface Extended Energy Loss Fine Structures (SEELFS) have been detected above the magnesium ionization K edge of γ-Al_2O_3-supported MgO at different loadings. Using a EXAFS-like data analysis procedure, the Fourier transforms of the first derivative energy loss spectra of samples at different MgO loading were obtained. From the Fourier functions it can be seen that with the increase of the MgO loading the peaks around 2.7 Å attributable to the Mg−Mg shell increased obviously in their peak heights and decreased slightly in their peak positions, whereas there were no significant differences in those of the peaks around 1.7 Å due to the Mg−O shell. When the MgO loading reached or exceeded the utmost dispersion capacity with the value of 0.17 g MgO/g Al_2O_3, which was determined by XRD in other paper,[17] the peaks of both types were in agreement with those of pure polycrystalline MgO. These semiquantitative results in coordination distances and the qualitative analysis in coordination numbers show that the coordination structures of Mg−O shells within MgO are not changed by the dispersion of MgO onto Al_2O_3 while those of Mg−Mg shells whose MgO loadings are lower than the threshold are changed greatly. The accessibility of a single experimental apparatus (an electron gun

and an auger analyzer) and low electron-penetrating depth (5−20 Å) of the SEELFS technique demonstrates its possible use in the research of surface science.

Acknowledgment. We thank Dr. Zhaiwei Liu for the collection and analysis of the SEELFS data. This work was financially supported by the National Natural Science Foundation of China (No.29733080) and National Climb Projects.

References and Notes

(1) Nakatsuka, T.; Kawasaki, H.; Yamashita, S.; Kohjiya, S. *Bull. Chem. Soc. Jpn.* **1979**, *52*, 2449.
(2) Reichle, W. T. J. *Catal.* **1985**, *94*, 547.
(3) Suzuki, E.; Ono, Y. *Bull. Chem. Soc. Jpn.* **1988**, *61*, 1008.
(4) Rao, K. K.; Gravelle, M.; Valente, J. S.; Figueras, F. *J. Catal.* **1998**, *173*, 115.
(5) Velu, S.; Swamy, C. S. *Appl. Catal. A* **1994**, *119*, 241.
(6) Cativiela, C.; Figueras, F.; Garcia, J. I.; Mayoral, J. A.; Zurbano, M. M. *Synth. Commun.* **1995**, *25*, 1745.
(7) Santhanalakshmi, J.; Raja, T. *Appl. Catal.* **1996**, *147*, 69.
(8) Corma, A.; Martin-Aranda, R. M. *Appl. Catal. A* **1993**, *105*, 271.
(9) Corma, A.; Iborra, S.; Primo, J.; Rey, F. *Appl. Catal. A* **1994**, *114*, 215.
(10) Choudary, B. M.; Narender, N.; Bhuma, V. *Synth. Commun.* **1995**, *25*, 2829.
(11) Kumbhar, P. S.; Sanchez-Valente, J.; Figueras, F. *Chem. Commun.* **1998**, 1091.
(12) Kumbhar, P. S.; Sanchez-Valente, J.; Lopez, J.; Figueras, F. *Chem. Commun.* **1998**, 535.
(13) Basu, B.; Satapathy, S.; Bhatnagar, A. K. *Catal. Rev.—Sci. Eng.* **1993**, *35*, 571.
(14) Hattori, H. *Chem. Rev.* **1995**, *95*, 537.
(15) Xie, Y. C.; Tang, Y. Q. *Adv. Catal.* **1990**, *37*, 1.
(16) Xie, Y. C.; Zhu, Y. X.; Zhao, B. Y.; Tang, Y. Q. *Stud. Surf. Sci. Catal.* **1998**, *118*, 441.
(17) Jiang, D. E.; Zhao, B. Y.; Xie, Y. C. *Acta Physico-Chimica Sinica* **2000**, *16* (2), 105.
(18) Tsuji, H.; Yagi, F.; Hattori, H.; Kita, H. *J. Catal.* **1994**, *148*, 759.
(19) Shen, J. Y.; Kobe, J. M.; Chen, Y.; Dumesic, J. A. *Langmuir* **1994**, *10*, 3902.
(20) Ertl, G.; Küppers, J. *Low Energy Electrons and Surface Chemistry*, 2nd ed.; VCH Publishers: Weinheim, West Germany, 1985.
(21) Stern, E. A.; Sayers, D. E.; Lytle, F. W. *Phys. Rev. B* **1975**, *11*, 4836.
(22) Crescenzi, M. D.; Chiarello, G. *J. Phys. C* **1985**, 3595.
(23) Crescenzi, M. D. *Surf. Sci.* **1985**, *162*, 838.
(24) Crescenzi, M. D. *J. Vac. Sci. Technol. A* **1987**, *5*, 869.
(25) Crescenzi, M. D. *Surf. Sci. Rep.* **1995**, *21*, 89.